Optimal Correlations in Many-Body Quantum Systems

L. Amico,[1] D. Rossini,[2] A. Hamma,[3] and V. E. Korepin[4]

[1]*CNR-MATIS-IMM and Dipartimento di Fisica e Astronomia, Università di Catania,*
C/O ed. 10, viale A. Doria 6, I-95125 Catania, Italy
[2]*NEST, Scuola Normale Superiore and Istituto Nanoscienze-CNR, Piazza dei Cavalieri 7, I-56126 Pisa, Italy*
[3]*Perimeter Institute for Theoretical Physics, 31 Caroline Street North, Waterloo, Ontario N2L 2Y5, Canada*
[4]*C.N. Yang Institute for Theoretical Physics, State University of New York at Stony Brook, New York, New York 11794-3840, USA*

Information and correlations in a quantum system are closely related through the process of measurement. We explore such relation in a many-body quantum setting, effectively bridging between quantum metrology and condensed matter physics. To this aim we adopt the information-theory view of correlations and study the amount of correlations after certain classes of positive-operator-valued measurements are locally performed. As many-body systems, we consider a one-dimensional array of interacting two-level systems (a spin chain) at zero temperature, where quantum effects are most pronounced. We demonstrate how the optimal strategy to extract the correlations depends on the quantum phase through a subtle interplay between local interactions and coherence.

PACS numbers: 03.67.Mn, 03.65.Ta, 05.30.Rt, 75.10.Pq

The relation between correlations and measurement is well known in quantum metrology, where the optimal measurement strategy to extract information has been thoroughly investigated [1,2]. In that context positive-operator-valued measurements (POVMs) and information-ally complete (IC) measurements are of particular importance since, contrary to simple projective measurements, they allow a complete tomography of the quantum state [3]. They have been playing an important role also in foundational aspects of quantum mechanics and quantum information science, as well as in the physics of dissipative systems [4–7].

In this Letter we aim at establishing a bridge between quantum metrology and quantum many-particles physics. We consider subsystems A and B in a many-body ground state and analyze the correlations resulting from POVMs performed on one of them, say B. Emphasis will be devoted to the optimal correlations, namely the maximal amount of correlations established between A and B. We observe that performing a POVM on a given physical system is equivalent to performing a projective measurement on an enlarged system where the original one is coupled with a given "ancilla" (Naimark's theorem). Such an ancilla can be an appropriate subsystem, and then analyzing correlations induced by a POVM on a local degree of freedom, say B, is an effective way to study correlations of higher order (spin-block correlations). Equivalently, the ancilla can be a suitable environment entangled to the system, and then correlations can give precious information on the decoherence of the state of the local constituent A.

The total amount of correlations in any bipartite (mixed) quantum state $\hat{\rho}_{AB}$ is given by the mutual information: $I_{AB} \equiv \mathcal{S}(\hat{\rho}_A) + \mathcal{S}(\hat{\rho}_B) - \mathcal{S}(\hat{\rho}_{AB})$, where $\mathcal{S}(\hat{\rho}) = -\text{Tr}[\hat{\rho}\log_2\hat{\rho}]$ is the von Neumann entropy. A central

quantity we will address below is the quantum conditional entropy $\mathcal{S}_\mathcal{C}$, quantifying the ignorance about the composite system AB, once subsystem B has been measured with a generic POVM $\{\hat{B}_k\}$,

$$\mathcal{S}_\mathcal{C}(\hat{\rho}_{AB}|\{\hat{B}_k\}) = \sum_k p_k S(\hat{\rho}_{AB}^{(k)}). \qquad (1)$$

Here $\hat{\rho}_{AB}^{(k)}$ denotes the state of the composite system AB, conditioned to a given outcome of $\hat{B}_k$: $\hat{\rho}_{AB}^{(k)} = \frac{1}{p_k}[(\hat{\mathbb{I}} \otimes \hat{B}_k)\hat{\rho}_{AB}]$ with $\hat{\mathbb{I}}$ denoting the identity operator on the subsystem A and $p_k = \text{Tr}[(\hat{\mathbb{I}} \otimes \hat{B}_k)\hat{\rho}_{AB}]$. The global amount $\mathcal{C}_{AB}$ of optimal (classical) correlations between constituents A and B is established after applying a set of measurements on B that least disturbs part A,

$$\mathcal{C}_{AB} = \max_{\{\hat{B}_k\}}[\mathcal{S}(\hat{\rho}_A) - \mathcal{S}_\mathcal{C}(\hat{\rho}_{AB}|\{\hat{B}_k\})], \qquad (2)$$

where the maximization is with respect to the measurement strategy. The quantum discord [8] quantifies the amount of quantum correlations and is defined as the difference between total and classical ones: $\mathcal{Q}_{AB} = I_{AB} - \mathcal{C}_{AB}$. The maximization in Eq. (2) is generally a daunting task, since the optimization procedure has to be performed on the whole set of possible POVMs.

We apply the above notions to the case where A and B are individual spins of a quantum spin chain and consider both von Neumann projective measurements $\hat{M}_{\text{proj}}$ and generalized POVMs $\hat{M}_{\text{POVM}}$ [9]. We design a strategy to exploit the information input given by the physical system hosting the two spins. Namely, we assume that the symmetry of the POVM is fixed by the symmetry of the local interactions occurring in the physical system. However, we shall see this is not enough to optimize correlations, as the

coherence of the many-body system is going to play a major role.

Models and measurements.—As many-body systems, we consider a one-dimensional array of spins 1/2 interacting anisotropically along the three spatial directions with interaction strengths J_x, J_y, and J_z, and subjected to a uniform external field h. The Hamiltonian reads

$$\hat{\mathcal{H}} = \sum_i (J_x \hat{\sigma}_i^x \hat{\sigma}_{i+1}^x + J_y \hat{\sigma}_i^y \hat{\sigma}_{i+1}^y + J_z \hat{\sigma}_i^z \hat{\sigma}_{i+1}^z) - h \sum_i \hat{\sigma}_i^z, \quad (3)$$

where $\hat{\sigma}_i^\alpha$ ($\alpha = x, y, z$) are the Pauli matrices on site i. Hereafter we set $|J_x| = 1$ as the energy scale and work in units of $\hbar = 1$. At zero temperature, different quantum phases can exist, separated by quantum phase transitions (QPTs) [12]. Moreover, a completely factorized ground state may occur at a specific value of the field h_f [13]. For *xyz* spin chains of Eq. (3), this is given by $h_f = 2\sqrt{(1 - J_z)(J_y - J_z)}$ [14].

We will discuss Eq. (3) in the following cases: (I) The ferromagnetic Ising chain ($J_y = J_z = 0$, $J_x = -1$), which undergoes a QPT at $h_c = 1$, and factorization at $h_f = 0$. It can be experimentally realized with the magnetic compound $CoNb_2O_6$ [15]. (II) The nonintegrable antiferromagnetic *xyx* model ($J_x = J_z = 1$), with $J_y = 1/4$ (this is the case experimentally realized with Cs_2CoCl_4 [16]). Such model displays a QPT at $h_c \simeq 3.21$ and factorization at $h_f \simeq 3.16$. (III) The antiferromagnetic anisotropic *xxz* Heisenberg chain ($J_x = J_y = 1$) with $J_z = 1/2$. At zero field it presents a critical *xy* phase with quasi-long-range order (quasi-LRO) for $|J_z| < 1$; this is separated by two classical phases with QPTs at $J_z = \pm 1$. For $h \neq 0$, the *xy* phase is a strip in the phase diagram, eventually turning into polarized phases for sufficiently strong magnetic field (the factorization phenomenon degenerates in the saturation occurring as a first-order transition). Despite local interactions being clearly different, both the quantum Ising and *xyx* models display an Ising-like QPT with Z_2-symmetry breaking; the *xxz* model, instead, is characterized by a critical phase without order parameter.

We first deal with standard projective measurements $\hat{M}_{\text{proj}} = \{\hat{B}_\pm\}$ along the field direction, defined by $\hat{B}_\pm = \frac{1}{2}(\hat{\mathbb{1}} \pm \hat{\sigma}^z)$. Then we engineer a more sophisticated set of POVMs, such that the symmetry of the measurement keeps track of local interactions between the spins. Specifically, we look at the interactions J_x, J_y, J_z entering Eq. (3), and design the following $\hat{M}_{\text{POVM}} = \{\hat{B}_k\}$:

$$\hat{B}_k = \frac{1}{4}(\hat{\mathbb{1}} + \vec{a}_k \cdot \hat{\vec{\sigma}}), \qquad k = 1, \dots, 4, \quad (4)$$

where $\hat{\vec{\sigma}} = (\hat{\sigma}^x, \hat{\sigma}^y, \hat{\sigma}^z)$ and $\vec{a}_k$ is such that $\vec{a}_1 = \alpha(J_x, J_y, J_z)$, $\vec{a}_2 = \alpha(J_x, -J_y, -J_z)$, $\vec{a}_3 = \alpha(-J_x, J_y, -J_z)$,
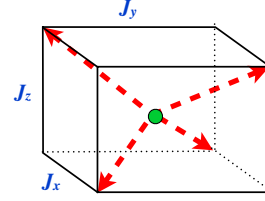

FIG. 1 (color online). The four vectors entering the POVM measurement of Eq. (4). They point from the center to non-adjacent corners of a parallelepiped with edges fixed by the anisotropic interaction occurring into the system.

$\vec{a}_4 = \alpha(-J_x, -J_y, J_z)$, and $\alpha^{-1} = \sqrt{J_x^2 + J_y^2 + J_z^2}$ (see Fig. 1). For generic J_α, $\hat{M}_{\text{POVM}}$ will be denoted as coupling-oriented informationally complete (CIC) POVM. The choice of the vectors $\vec{a}_k$ in Eq. (4) reflects the symmetry of the Hamiltonian by changing $J_\alpha \to -J_\alpha$ by $\hat{U} \hat{\mathcal{H}} \hat{U}^\dagger$, with $\hat{U}^\alpha = \prod_i \hat{\sigma}_{2i+1}^\alpha$. In the isotropic case $J_x = J_y = J_z$, the POVM in Eq. (4) degenerates in a symmetric information-ally complete (SIC) POVM [5]. We comment that all the $\hat{B}_k$ do not depend on the external field explicitly. We shall see that such a dependence enters in a subtle way related to the macroscopic order of the system.

In order to compute the amount of correlations between any two spins at distance $r \equiv |A - B|$, one needs to access the single- and two-spin reduced density matrices $\hat{\rho}_A$ and $\hat{\rho}_{AB}$. Hereafter, we focus on the symmetry-broken ground states of the Hamiltonian in Eq. (3), which is symmetric under a global phase flip along the z-axis [17]. We observe that the generic two-site reduced density matrices of such states are beyond the so called "*X*-state" structure (emerging in symmetric states, and for which expressions for quantum and classical correlations are known [18]). Therefore, in the present case, in principle the optimal correlations might be achieved beyond projective measurements [11]. To access all the required two-point correlators, we resort to the density matrix renormalization group approach with open boundary conditions [19]. We consider sufficiently long chains, such to reduce unwanted edge effects and to approach the ideal thermodynamic limit. For the Ising and the *xyx* model, we add a small longitudinal field $h_x \sim 10^{-6}$ along the *xy* plane to ensure the Z_2-symmetry breaking.

Comparison between different measurement strategies.—We start our analysis by presenting results obtained for the quantum conditional entropy $\mathcal{S}_\mathcal{C}^{(r)}$ in Eq. (1), probing how the local interactions affect the measurement, without any further optimization. Figure 2 displays $\mathcal{S}_\mathcal{C}^{(1)}$ for two neighboring spins respectively for the Ising model, the *xyx* model and the *xxz* model in a transverse field h. The total amount of correlations reflects the main properties of the ground state: in particular the peaks denote QPT points that are associated to a divergence in their first derivative, while factorization fields are marked by the vanishing of all correlations. In all the three considered spin systems,
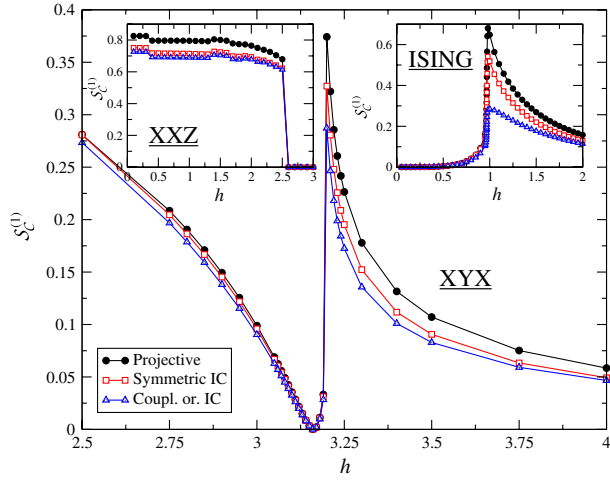
FIG. 2 (color online). Conditional entropy $\mathcal{S}_\mathcal{C}^{(1)}$ for the three cases: (I) Ising, (II) xyx, and (III) xxz model in an external field [see Eq. (3)]. Correlations are considered between two nearest neighbors at the center of the chain ($r = 1$); the length of the chain is $L = 200$. The various curves correspond to different measurement strategies on subsystem B: standard projective measurement along the z direction (black circles), SIC POVM (red squares), as well as IC POVM set by the specific interactions of the model (blue diamonds).

measurement performances decrease from the CIC POVM to the SIC POVM and to the projective measurement along the computational basis z.

Much larger amounts of correlations can be achieved by performing suitable optimization strategies on the measurements considered above. In the following, we apply two different kinds of optimization: (I) We rotate the direction of the elements $\hat{B}_k$ of the projective measurement $\hat{M}_{\mathrm{proj}}$ and of the POVM $\hat{M}_{\mathrm{POVM}}$ on the Bloch sphere, by keeping the angles between the vectors $\vec{a}_j$ constant (this corresponds to a rigid rotation of the experimental apparatus); optimal correlations are thus obtained by maximizing over the angles (θ, ϕ) entering the rotation. (II) In the case of CIC POVM, we independently vary the three parameters J_x, J_y, and J_z, defining the direction of the vectors $\vec{a}_k$ in $\hat{M}_{\mathrm{POVM}}$ (see Fig. 1) [20].

In Fig. 3 we display the classical correlations between two neighboring spins for the three considered models by adopting the optimizations discussed above. Similarly to the quantum conditional entropy, $\mathcal{C}^{(r=1)}$ displays a noticeable dependence on the model and on the magnetic field. While in the Ising model the CIC angle-dependent POVM and projective measurement give the same answer, for the xyx and xxz model the angle-dependent strategy is not optimal and is outperformed by the projective measurements. The three-parameter (3P) POVM optimizations provide the same correlations of the projective measurements in the disordered regions and in xxz model; however, where the order parameter $\langle\sigma^x\rangle \neq 0$, they are still worse than the projective measurement.
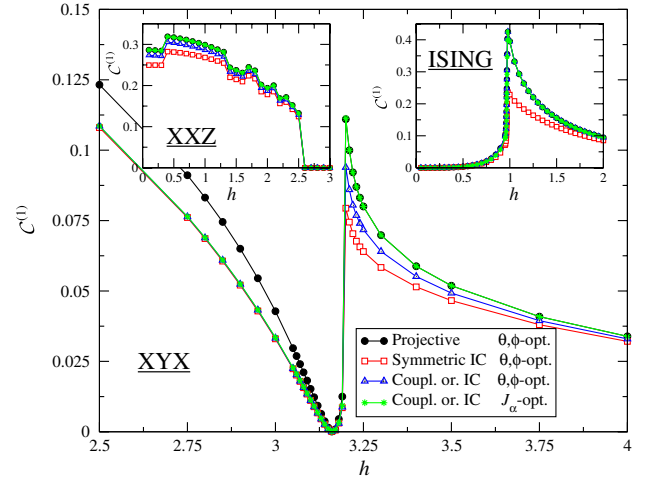

FIG. 3 (color online). Same as in Fig. 2, but for the classical correlations $\mathcal{C}^{(1)}$ optimized over the given measurement strategy. In the first three cases, projective measurement, SIC POVM and IC POVM (see the symbol pattern of Fig. 2), the optimization in Eq. (2) is performed on the rotation angles (θ, ϕ) of the Bloch sphere of subsystem B. The green stars refer to IC POVM optimized by varying the three parameters J_α defining the direction of the vectors $\vec{a}_k$.

A similar analysis of correlations for $r > 1$ strongly suggests that the effect of different measurement strategies at long ranges vanishes everywhere but close to the quantum critical points, where the correlation functions decay algebraically with r (Fig. 4).

In the disordered phase of the Ising and the xyx model, where the order parameter $\langle\hat{\sigma}^x\rangle = 0$, as well as in the xxz model, θ_{opt} and ϕ_{opt} are fixed to a value independent by h (see Table I). By analyzing the rotated measurements $\hat{B}_k(\theta, \phi)$, it turns out that projective measurements can achieve a local measurement along the eigenvectors $|v\rangle$ of $\hat{\sigma}_{\mathrm{loc}} = J_x\hat{\sigma}^x + J_y\hat{\sigma}^y + J_z\hat{\sigma}^z$, fixed by the system
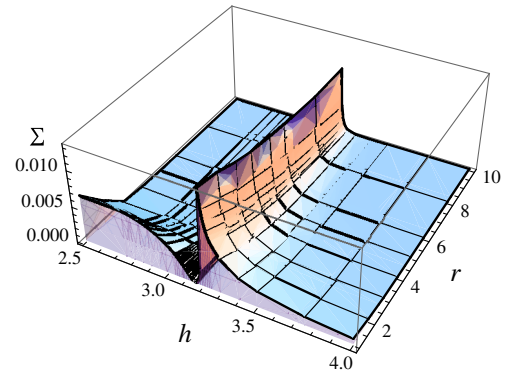

FIG. 4 (color online). Quadratic difference between the optimal correlations obtained following the four different measurement strategies $\hat{M}$ described above (see also Fig. 3): $\Sigma^2 \equiv \sum_{\hat{M}}(\mathcal{C}^{(r)} - \langle\mathcal{C}^{(r)}\rangle)^2$. Here $\langle\mathcal{C}^{(r)}\rangle$ denotes the average correlation with respect to the four $\hat{M}$. Data are shown for the xyx model as a function h and for different $r = |A - B|$.

TABLE I.   Optimization angles $\theta_{opt} \in [0, \pi]$ and $\phi_{opt} \in [0, 2\pi)$ in the disordered phases with vanishing order parameter. k is any integer positive number. In the last line: optimization directions J_α for CIC measures.

	Ising, $h > h_c$	xyx, $h > h_c$	xxz, quasi-LRO
Proj.	$\theta_1 = \pi/2$; $\phi_1 = 0$	$\theta_1 = \pi/2$; $\phi_1 = 0$	$\theta = \pi/2$; $\forall\ \phi$
	$\theta_2 = \theta_1$; $\phi_2 = \pi$	$\theta_2 = \theta_1$; $\phi_2 = \pi$	
CIC	$\theta_1 = 0$; $\forall\ \phi_1$	$\theta_k = \pi$	$\theta = 0$; $\forall\ \phi$
	$\theta_2 = \pi$; $\phi_2 = 0, \pi$	$\phi_k \approx 1.478 + k\pi/2$	
	$\forall\ \theta_3$; $\phi_3 = \pi/2 + k\pi$		
SIC	$\theta_k = \pi$	$\theta_k = \pi$	$\theta_{k_1} \approx 0.955$; $\phi_{k_1} = 3\pi/4 + k_1\pi$
	$\phi_k \approx 0.393 + k\pi/2$	$\phi_k \approx 1.152 + k\pi/2$	$\theta_{k_2} \approx 2.185$; $\phi_{k_2} \approx 3.92 + k_2\pi$
3P CIC	$J_x = 1$; $J_y = J_z = 0$	$J_x = 1$; $J_y = J_z = 0$	$J_z = 0$; $\forall\ (J_x, J_y)$

Hamiltonian. For both the xyx and Ising model, optimal correlations are attained by using projective measurements along the x axis: $\hat{B}_\pm(\pi/2, 0) = \frac{1}{2}(\hat{\mathbb{1}} \pm \hat{\sigma}^x)$. This reflects the Z_2-symmetry $\sigma^x \rightarrow -\sigma^x$ of the paramagnetic phase. On the other hand, the operators of each optimized four-element POVM can be written as $\hat{B}_k(\theta_{opt}, \phi_{opt}) = |\psi_k^{opt}\rangle\langle\psi_k^{opt}|$, where $|\psi_k^{opt}\rangle$ is of the type $|\psi_k^{opt}\rangle = \xi_k\sqrt{1 - a_z}e^{2i\phi_{opt}}|\uparrow\rangle + \sqrt{1 + a_z}|\downarrow\rangle$, with $\xi_k \in \mathbb{C}$. It turns out that $|\psi_k^{opt}\rangle = |v\rangle$ with $\phi_{opt} = 0$ and $\xi_k = \xi^{(v)} = e^{i\arg(a_x + ia_y)}$ for projective measurements. For CIC measurements $\xi_k = \xi^{(v)}$, but $\phi \neq 0$; for SIC-POVM $\xi_k \neq \xi^{(v)}$. We note that for large h, where the state is nearly fully polarized along z, correlations are vanishing and therefore measurements along any direction are optimal. The CIC with 3P optimization leads to optimal correlations in the disordered phase.

In the symmetry-broken phase, optimal angles $(\theta_{opt}, \phi_{opt})$ for both Ising and xyx models display a nontrivial dependence on the order parameter, as visible in Fig. 5.
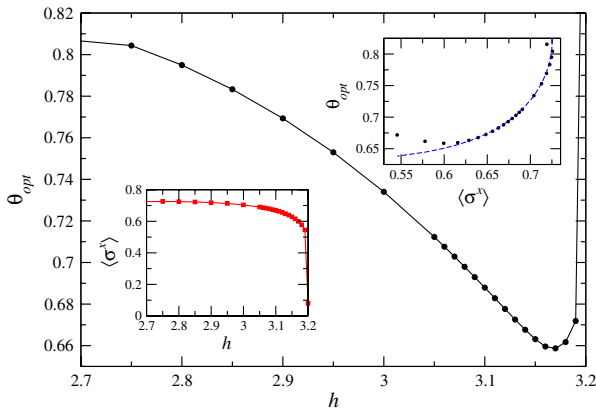

FIG. 5 (color online).   Optimization parameters for the nearest-neighbor correlations in the xyx model, after a projective measurement. The fit in the upper inset (dashed blue line) is $\theta_{opt} = 0.824 - 0.709\sqrt{0.0769 - x^8}$. The other optimization strategies are discussed in the Supplemental Material [21]. In the lower inset we display the order parameter $\langle\hat{\sigma}^x\rangle$ as a function of h, as extracted from numerical simulations.

Except for a region close to the QPT, we fitted our results using the formula $\theta_{opt} = A\sqrt{B - \langle\hat{\sigma}^x\rangle^n} + k$, where the parameters A, B, k are model-dependent, while we imposed $n = 8$, inspired by the linear variation of θ_{opt} with h that we observed in the Ising model, and by the characteristic exponent $\beta = 1/8$ of its order parameter at the QPT (see the upper inset of Fig. 5). In some cases we found significant deviations from such dependence (see Supplemental Material [21] for a detailed discussion of the optimal parameters). Peculiar behaviors arise close to the QPT, where dramatic changes appear, and to the factorization points, where an extremal value is reached. Such behavior is consistent with the interpretation of the factorization phenomenon as a "correlation transition" resulting from a competition between parallel and antiparallel entanglement [22,23]: Optimal correlations arise from the balance of two optimizations involving the parallel and antiparallel entangled components (both present in the ground state). The two entanglement components switch each other and an extremal optimal angle is reached at h_f.

It is interesting to compare the optimal angles in the Z_2 symmetry-broken phase with those in the xy gapless phase of the xxz model, where the order parameter is vanishing in a nontrivial way because correlations decay algebraically. For both projective and CIC measurements, the optimization in such phase is characterized by a fixed value of θ_{opt}, $\forall\ \phi_{opt}$, thus indicating that, because of quasi-LRO, any preferential measurement direction is not unique in the phase. Such a scenario is confirmed by the 3P optimized CIC POVM (last row of Table I).

Discussion.—We analyzed spin-spin correlations that are established after performing a local measurement on one of the two spins in the ground state of a quantum spin chain. We considered projective measurements as well as symmetric IC POVMs; furthermore, we engineered coupling-oriented IC POVMs with the aim to shed light on how the optimal measurement can be performed *a priori*, once a certain knowledge on the system has been previously acquired. The measurement protocols were first tested, without regard for adjustable parameters, by looking at the conditional entropy. Then we focused on the possibility to adjust the measurement on the basis of local interactions.

Interactions, coherence, and symmetry fix the "optimal flow" of information; the optimal strategy to extract the correlations eventually depends on the quantum phase.

Specifically, an analysis of the quantum Ising and the xyx model, both sharing the same kind of Z_2-symmetry-breaking QPT (even if with very different local interactions), showed that in the ordered phase, the optimal correlation follows the global order, in the sense that the parameters characterizing the optimal measurement strategy vary with the exponent β of the order parameter. Such a result also could be useful to heuristically dictate the optimal measurement strategy for higher order correlations (between spin-blocks), where the optimization protocol is not practicable. On the contrary, in the disordered phase, local interactions fix the optimal strategy, in the sense that optimal correlations are attained by fulfilling a local requirement of projecting along σ_{loc}. The results on the xxz model further support this scenario: optimal correlations are obtained for measurements respecting the in-plane symmetry of the model for any fixed direction in the xy plane (there is no preferential direction because of quasi-LRO in the xy critical phase).

Finally, we analyzed correlations at long ranges showing that, near the QPT, long-range correlations are strongly affected by the measurement strategies (see Fig. 4). In the gapped phase any measurement strategy produces the same result, on a length-scale where the correlation functions themselves are sensible.

Given the relation between optimal correlations and quantum discord, our results could be important in many-body implementations of quantum information protocols. We also comment that, being a single-spin state fully accessible through Eq. (4), our scheme provides an effective strategy to perform state tomography of one of the two spins (a notoriously challenging problem in quantum magnets).

[1] E. Prugovecki, Int. J. Theor. Phys. **16**, 321 (1977).
[2] V. Giovannetti, S. Lloyd, and L. Maccone, Nature Photon. **5**, 222 (2011).
[3] A. Peres, *Quantum Theory: Concepts and Methods* (Kluwer, Dordrecht, 1993).
[4] P. Busch, Int. J. Theor. Phys. **30**, 1217 (1991).
[5] J. Řeháček, B.-G. Englert, and D. Kaszlikowski, Phys. Rev. A **70**, 052321 (2004).
[6] C. A. Fuchs, arXiv:quant-ph/0205039.
[7] G. M. D'Ariano, M. G. A. Paris, and M. F. Sacchi, Adv. Imag. Electr. Phys. **128**, 205 (2003).
[8] H. Ollivier and W. H. Zurek, Phys. Rev. Lett. **88**, 017901 (2001); L. Henderson and V. Vedral, J. Phys. A: Math. Gen. **34**, 6899 (2001).
[9] For spin-spin correlations, the optimization in Eq. (2) can be constrained to four-projector-element POVMs [10]. Though von Neumann measurements were proved to be more effective than three-element POVMs, there is no conclusive proof for the efficiency of four-element POVMs [11]. The optimization within four-element POVMs would involve eleven raw parameters.
[10] G. M. D'Ariano, P. Lo Presti, and P. Perinotti, J. Phys. A **38**, 5979 (2005).
[11] S. Hamieh, R. Kobes, and H. Zaraket, Phys. Rev. A **70**, 052325 (2004).
[12] S. Sachdev, *Quantum Phase Transitions* (Cambridge University Press, Cambridge, England, 2001).
[13] J. Kurmann, H. Thomas, and G. Müller, Physica A (Amsterdam) **112**, 235 (1982); T. Roscilde, P. Verrucchi, A. Fubini, S. Haas, and V. Tognetti, Phys. Rev. Lett. **94**, 147208 (2005); L. Amico, F. Baroni, A. Fubini, D. Patanè, V. Tognetti, and P. Verrucchi, Phys. Rev. A **74**, 022322 (2006).
[14] S. M. Giampaolo, G. Adesso, and F. Illuminati, Phys. Rev. Lett. **100**, 197201 (2008); Phys. Rev. B **79**, 224434 (2009).
[15] R. Coldea, D. A. Tennant, E. M. Wheeler, E. Wawrzynska, D. Prabhakaran, M. Telling, K. Habicht, P. Smeibidl, and K. Kiefer, Science **327**, 177 (2010).
[16] M. Kenzelmann, R. Coldea, D. A. Tennant, D. Visser, M. Hofmann, P. Smeibidl, and Z. Tylczynski, Phys. Rev. B **65**, 144432 (2002).
[17] O. F. Syljuåsen, Phys. Rev. A **68**, 060301(R) (2003); A. Osterloh, G. Palacios, and S. Montangero, Phys. Rev. Lett. **97**, 257201 (2006); T. R. de Oliveira, G. Rigolin, M. C. de Oliveira, and E. Miranda, Phys. Rev. A **77**, 032325 (2008).
[18] M. Ali, A. R. P. Rau, and G. Alber, Phys. Rev. A **81**, 042105 (2010).
[19] U. Schollwöck, Rev. Mod. Phys. **77**, 259 (2005).
[20] The effect of such operations in the energy spectrum of the system was discussed by S. M. Giampaolo, F. Illuminati, P. Verrucchi, and S. De Siena, Phys. Rev. A **77**, 012319 (2008).
[21] See Supplemental Material at http://link.aps.org/supplemental/10.1103/PhysRevLett.108.240503 for a more detailed discussion on the optimal angles, as well as on the optimal vectors, which maximize the correlations in the symmetry-broken ordered phase.
[22] A. Fubini, T. Roscilde, V. Tognetti, M. Tusa, and P. Verrucchi, Eur. Phys. J. D **38**, 563 (2006).
[23] B. Tomasello, D. Rossini, A. Hamma, and L. Amico, Europhys. Lett. **96**, 27002 (2011).